The PP-motif in luminal loop 2 of ZnT transporters plays a pivotal role in TNAP activation

Shigeyuki Fujimoto[*], **Tokuji Tsuji**[*], **Takashi Fujiwara**[†], **Taka-aki Takeda**[*], **Chengfeng Merriman**[‡], **Ayako Fukunaka**[*,1], **Yukina Nishito**[*], **Dax Fu**[‡], **Eitan Hoch**[§], **Israel Sekler**[§], **Kazuhisa Fukue**[*], **Yusaku Miyamae**[*], **Seiji Masuda**[*], **Masaya Nagao**[*], and **Taiho Kambe**[*,2]

[*]Division of Integrated Life Science, Graduate School of Biostudies, Kyoto University, Kyoto 606-8502, Japan

[†]Laboratory of Cell Dynamics, Graduate School of Bioagricultural Sciences, Nagoya University, Nagoya 464-8601, Japan

[‡]Department of Physiology, Johns Hopkins School of Medicine, Baltimore, MD 21205, U.S.A

[§]Department of Physiology, Faculty of Health Sciences, Ben-Gurion University, Beer-Sheva 84105, Israel

Abstract

Secretory and membrane-bound zinc-requiring enzymes are thought to be activated by binding zinc in the early secretory pathway. One such enzyme, tissue-non-specific alkaline phosphatase (TNAP), is activated through a two-step mechanism, via protein stabilization and subsequent enzyme activation through metalation, by ZnT5–ZnT6 heterodimers or ZnT7 homodimers. However, little is known about the molecular basis underlying the activation process. In the present study, we found that the di-proline motif (PP-motif) in luminal loop 2 of ZnT5 and ZnT7 is important for TNAP activation. TNAP activity was significantly reduced in cells lacking ZnT5–ZnT6 heterodimers and ZnT7 homodimers [triple knockout (TKO) cells]. The decreased TNAP activity was restored by expressing hZnT5 with hZnT6 or hZnT7, but significantly less so (almost 90% less) by expressing mutants thereof in which the PP-motif was mutated to alanine (PP-AA). In TKO cells, overexpressed hTNAP was not completely activated, and it was converted less efficiently into the holo form by expressing a PP-AA mutant of hZnT5 with hZnT6, whose defects were not restored by zinc supplementation. The zinc transport activity of hZnT7 was not significantly impaired by the PP-AA mutation, indicating that the PP-motif is involved in the TNAP maturation process, although it does not control zinc transport activity. The PP-motif is highly conserved in ZnT5 and ZnT7 orthologues, and its importance for TNAP activation is

conserved in the *Caenorhabditis elegans* hZnT5 orthologue CDF5. These results provide novel molecular insights into the TNAP activation process in the early secretory pathway.

Keywords

early secretory pathway; PP-motif; TNAP; zinc-requiring enzyme; zinc transport; ZnT

INTRODUCTION

Zinc plays crucial roles in many biological processes, in which it is indispensable as a structural component, cofactor and signalling mediator in protein functions [1-4]. Recent *in silico* analyses indicate that approximately 3000 proteins have a putative zinc-binding motif [5]. Thus, zinc homoeostasis and metabolism are strictly regulated by a number of proteins at systemic and cellular levels [4,6]. Two zinc transporter families, Zn transporter [ZnT, solute carrier 30A (SLC30A)] and Zrt, Irt-like protein (ZIP, SLC39A), operate as essential components to control these processes by transporting zinc across cellular membranes [3,4,7-13]. ZnT transporter functions have been more extensively investigated at the molecular level [9,11] because the 3D structure and the zinc/proton exchange transport mechanism have been resolved in the bacterial ZnT homologue YiiP [14-17], thus many mutagenesis studies have been performed in ZnT transporters and their homologues [18-26]. In these studies, many amino acid residues have been shown to be involved in zinc transport and determining metal specificity [18-22]. However, little is known about the amino acid residues or motifs that are associated with other functions of ZnT transporters.

Most ZnT transporters have crucial functions in transporting zinc into intracellular organelles and vesicles [9,27-29]. Among them, ZnT5, ZnT6 and ZnT7 are thought to play key roles in transporting zinc into the early secretory pathway to activate zinc-requiring enzymes that are secreted out of cells or that reside within intracellular organelles, as well as in maintaining the homoeostasis of secretory pathway functions [9,27,30]. Thus far, we have shown that ZnT5 and ZnT6 form heterodimers (in which ZnT6 operates as an auxiliary subunit) and ZnT7 forms homodimers [19,31,32], and that these two ZnT transport complexes activate zinc-requiring enzymes such as tissue-non-specific alkaline phosphatase (TNAP) [27,31,33]. The TNAP activation process is intricately regulated. Cytosolic zinc is probably transferred to ZnT5–ZnT6 heterodimers and ZnT7 homodimers, in which ZnT1, ZnT4 and metallothionein (MT) probably play important co-operative roles [6,21,34]. Moreover, TNAP is activated by ZnT5–ZnT6 heterodimers or ZnT7 homodimers in an elaborate two-step mechanism in which TNAP is first stabilized by either complex, and then is subsequently activated via metalation by zinc, which is supplied by either complex [6,34,35]. However, the molecular basis of these processes is unknown. In the present study, we document that the di-proline motif (PP-motif) in luminal loop 2 of hZnT5 and hZnT7 [note that luminal loop 6 in hZnT5, which has 15 putative transmembrane domains (TMDs), corresponds to luminal loop 2 in other ZnT transporters, including hZnT7, which have six TMDs that constitute a cation efflux domain [36], but 'luminal loop 2' is used for hZnT5 and its orthologues as a matter of practical convenience in this paper], which is highly conserved in ZnT5 and ZnT7 orthologues, is important for TNAP activation. Our results

provide molecular insights into how and why ZnT5–ZnT6 heterodimers and ZnT7 homodimers can fully activate TNAP in a specific manner. Thus, they suggest that the luminal motif of ZnT transporters makes an important contribution to their own unique functions.

EXPERIMENTAL

Cell culture and transfection

Chicken B-lymphocyte-derived DT40 cells, DT40 cells deficient in the *ZnT5*, *ZnT6* and *ZnT7* genes [*ZnT5⁻ ZnT6$^{-/-}$ ZnT7$^{-/-}$* triple knockout (TKO) cells], and DT40 cells deficient in the *ZnT1*, *MT* and *ZnT4* genes (*ZnT1$^{-/-}$ MT$^{-/-}$ ZnT4$^{-/-}$* cells) were maintained as described previously [33]. DNA transfection into DT40 cells was conducted as previously described [37]. More than three independent clones were established per transfectant in all experiments. Cell viability in high extracellular zinc concentrations was evaluated using *ZnT1$^{-/-}$ MT$^{-/-}$ ZnT4$^{-/-}$* cells [21,38]. The cells were cultured in the presence of 30–70 μM ZnSO$_4$ for 72 h, and viable cells were measured by the Alamar Blue assay (Trek Diagnostic Systems) as described previously [39].

Plasmid construction

Plasmids used for the expression of FLAG-tagged human ZnT5 (FLAG-hZnT5) and haemagglutinin (HA)-tagged human ZnT6 (HA-hZnT6), HA-hZnT7, hZnT4-HA and hTNAP were described previously [19,21,35]. Plasmids used to express FLAG-tagged CDF5 (FLAG-CDF5) and HA-tagged TOC1 (HA-TOC1) were constructed by inserting each cDNA into the pA-Puro and pA-Ecogpt vectors respectively. Fragments containing full-length cDNAs of CDF5 and TOC1 were amplified by reverse transcription–PCR using total RNA prepared from *Caenorhabditis elegans* as a template. Amplified cDNAs were sequenced in both directions. The plasmids used to express hZnT5, hZnT7, CDF5 and hZnT4 mutants were constructed by a two-step PCR method, followed by insertion into the pA-Puro vector. All plasmids were linearized with appropriate restriction enzymes prior to electroporation [37]. In growth assays of *Saccharomyces cerevisiae* mutants, hZnT7-HA and its mutants were inserted into the pYES2 vector (Invitrogen). The pYES2 vector containing *S. cerevisiae MSC2* (*ScMSC2*) was described previously [40].

Measurement of TNAP activity

Membrane proteins or total cellular protein extracts were prepared from cells that were lysed in ALP lysis buffer. Samples of 2–5 μg of membrane proteins or whole cell lysates were used to measure TNAP activity as described previously [37]. Calf intestine alkaline phosphatase (Promega) was used to make a standard curve [21].

Immunoblotting and immunoprecipitation experiments

Immunoblotting and immunoprecipitation were performed as described previously [37]. Briefly, blotted PVDF membranes (Millipore) were blocked with a solution of 4% (w/v) non-fat dried skimmed milk powder and 0.1 % Tween 20 in PBS prior to incubation with anti-FLAG-tag (anti-DDDDK; MBL; 1:3000 dilution), anti-HA HA-11 (Covance; 1:3000 dilution) or anti-TNAP (Santa Cruz Biotechnology; 1:3000 dilution) antibodies in blocking

solution. To control for loading, *S. cerevisiae* proteins that were separated by SDS/PAGE were silver-stained with 2D-Silver Stain Reagent II (Cosmo Bio). For immunoprecipitations, membrane proteins from cells that were lysed in NP-40 buffer were incubated with anti-FLAG M2 (Sigma–Aldrich; 1:200 dilution) or anti-HA HA-11 (1:200 dilution) antibodies for 1 h at 4 °C prior to the addition of 10 μl of Protein G–Sepharose beads (GE Healthcare) [38]. After an additional incubation for 12 h at 4 °C, immunoprecipitates were subjected to immunoblotting. Horseradish peroxidase-conjugated rabbit anti-mouse secondary antibodies (GE Healthcare) or TrueBlot anti-mouse IgG (eBioscience) were added at a 1:3000 dilution for protein detection. A fluoro-image was obtained using an LAS1000 Plus (Fujifilm) or LAS500 (GE Healthcare) gel documentation system.

Immunofluorescence staining

Immunostaining for wild-type (WT) hZnT5, hZnT6, CDF5 and TOC1, as well as mutants thereof, was performed as described previously [37]. Briefly, cells were stained with an anti-FLAG antibody (anti-DDDDK; MBL; 1:2000 dilution), followed by Alexa Fluor 488-conjugated goat anti-rabbit IgG (Molecular Probes; 1:200 dilution), or with anti-HA HA11 (Covance; 1:2000 dilution), followed by Alexa Fluor 594-conjugated goat anti-mouse IgG (Molecular Probes; 1:200 dilution). The stained cells were observed using a Zeiss Axioplan 2 microscope (Carl Zeiss) that was equipped with an Metamorph digital camera (Olympus), or a fluorescent microscope FSX100 (Olympus). Images were analysed using Adobe Photoshop CS.

Model structures of hZnT5, hZnT6 and hZnT7, and sequence similarity

Homology models of hZnT5, hZnT6 and hZnT7 were obtained using a Multiple Mapping Method [41]. The crystal structure of YiiP (PDB code 3H90) served as a structural template for modelling homologous mammalian targets. Manual inspection of structurally aligned protein pairs was used to discriminate between alternative alignment choices, and models were built by optimizing the positions of target residues that fold into the known YiiP 3D structural template. All graphic presentations were prepared using the program PyMOL (DeLano Scientific). The identity and similarity of CDF5 to hZnT5, hZnT7 and hZnT4 were evaluated using the National Center for Biotechnology Information Basic Local Alignment Search Tool server (http://www.ncbi.nlm.nih.gov/BLAST/).

Growth assay of an *S. cerevisiae* mutant

The *S. cerevisiae* mutant DY150 *msc2* (*MATa ade2 can1 his3 leu2 trp1 ura3 msc2::HIS3*) was transformed with the indicated plasmids using a lithium acetate/single-stranded carrier DNA/PEG method [42]. The transformed yeast cells were precultured in SRaf medium containing the appropriate amino acids for auxotrophy for 18 h at 30 °C, and diluted to an attenuance at 600 nm of 0.1 in SGal medium containing appropriate amino acids. After incubation for 1 h at 30 °C, aliquots (5 μl) of the suspension culture were spotted on to solid YPGEgal medium as described previously [40]. Plates were incubated for 3 days at 30 and 37 °C.

RESULTS

Analyses of the amino acid residues in the luminal loops of hZnT5 that are associated with TNAP activation

TNAP activity in TKO cells was not restored when human ZnT (hZnT) transporters, such as hZnT2, hZnT3 and hZnT8, were ectopically expressed, or when hZnT1 and hZnT4 were overexpressed, even if they partially (transiently) localized to the early secretory pathway [35]. Moreover, TNAP was stabilized by co-expressing hZnT5 and hZnT6, or by expressing hZnT7 prior to its activation [35]. Intriguingly, we found that a zinc transport-competent mutant hZnT5, in which the HDHD core motif of the intramembranous zinc-binding site is mutated to DDHD or HDHE, failed to activate TNAP in TKO cells when co-expressed with hZnT6 (Supplementary Figure S1). Considering these results, we speculated that hZnT5 and hZnT7 may have a specific sequence (motif) in their luminal loops that is associated with TNAP activation. To investigate this possibility, we used a site-directed mutagenesis strategy to modify luminal loops 1, 2 and 3 of hZnT5 (note that luminal loops 1, 2 and 3 in most ZnT transporters that contain six TMDs correspond to luminal loops 5, 6 and 7 in ZnT5 that contains 15 TMDs, but luminal loops 1, 2 and 3 are used as a matter of practical convenience). We mutated amino acid residues in luminal loops 1, 2 and 3 of hZnT5 that are completely conserved among hZnT5, hZnT7 and the *C. elegans* hZnT5 orthologue (CDF5, see below) (Figure 1A). Specifically, alanine-scanning mutagenesis was used to modify residues Y436, N441, G444, L445 and I446 in luminal loop 1, P514, P515 and L522 in luminal loop 2 and I607, S609, F616 and G617 in luminal loop 3 of hZnT5. T440 in luminal loop 1 was also mutated to alanine because a serine residue is present at this position in hZnT7. No mutants showed any extreme reduction in TNAP activity, except for the L445A, P514A and P515A mutants (approximately 30, 30 and 50 % reduction respectively), when they were stably co-expressed with hZnT6 in TKO cells, compared with that in TKO cells stably co-expressing WT hZnT5 and hZnT6 (Figures 1B-1D). Moreover, we mutated F435 in luminal loop 1, and Q615, F619 and I620 in luminal loop 3 of hZnT5, because the corresponding amino acid residues differ among hZnT7 and CDF5, and they are moderately conserved as valine, phenylalanine, tyrosine and lysine residues, respectively, in other ZnT transporters (Figure 1A). We examined the possibility that these residues might impair TNAP activation in other ZnT transporters, but TNAP activity was not significantly reduced in TKO cells when these mutants were stably co-expressed with hZnT6 (Figures 1B and 1D), which excludes this possibility. The protein expression levels of all of the hZnT5 mutants were almost the same as that of WT hZnT5 in TKO cells (Figures 1B–1D). Taken together, L445, P514 and P515 in the luminal loops may play pivotal roles in the activation of TNAP in the early secretory pathway.

The PP-motif in luminal loop 2 of hZnT5 is crucial for TNAP activation

We next examined the roles of two proline residues, P514 and P515 (a PP-motif), in luminal loop 2 of hZnT5, because the motif is uniquely conserved among hZnT5, hZnT7 and CDF5, as opposed to three other amino acids that occupy these positions in most other ZnT transporters (Figure 1A). To closely examine whether the PP-motif is crucial for TNAP activation, we again used a site-directed mutagenesis strategy to replace one or both proline residues with alanine in hZnT5. The hZnT5$_{PP-AA}$ mutant, in which the PP sequence was

replaced with AA, co-localized with hZnT6 (Figure 2A, upper panels) and formed a heterodimer with hZnT6, as did WT hZnT5 (Figure 2A, lower panels). Interestingly, TNAP activity was approximately 90 % lower in TKO cells that stably co-expressed the hZnT5$_{PP-AA}$ mutant and hZnT6, compared with that in cells that stably co-expressed WT hZnT5 and hZnT6 (Figure 2B). The protein expression levels were almost the same among the WT and mutants hZnT5 proteins, which excludes the possibility that the reduced TNAP activity in the cells resulted from a lower hZnT5 expression level in each mutant.

To investigate TNAP protein expression levels in TKO cells that stably co-express hZnT5$_{PP-AA}$ and hZnT6, we stably expressed hTNAP in these cells. The activity of hTNAP was moderately reduced (approximately 60 % less than that of TKO cells co-expressing WThZnT5 and hZnT6) (Figure 2C) compared with the endogenous TNAP activity, which was approximately 90 % less in TKO cells than in WT cells, as described in Figure 2(B). hTNAP proteins were detected as one major high-molecular-mass band corresponding to holo-hTNAP in TKO cells co-expressing WThZnT5 and hZnT6, whereas they were detected as one major high-molecular-mass and several minor lower-molecular-mass bands in TKO cells stably co-expressing hZnT5$_{PP-AA}$ and hZnT6. The low-molecular-mass bands probably correspond to apo-hTNAP, considering our previous results [30,35]. (In our previous report [30], the sizes of the major high-molecular-mass band and the minor lower-molecular-mass bands were calculated to be ~80 and ~60-kDa, but they were detected as ~75 and ~65-kDa bands, respectively, because a different protein size marker was used and the percentage of polyacrylamide in the gel differed.) The amounts of the low-molecular-mass bands were not significantly changed when protein degradation via the proteasome and lysosome was inhibited by treatment with MG132 and bafilomycin A1 (Figure 2C). Moreover, zinc supplementation did not fully restore hTNAP activity, and it did not alter the appearance of the low-molecular-mass bands (Figure 2D). These results suggest that the low-molecular-mass bands were unlikely to be derived from insufficient zinc transport by a heterodimer of hZnT5$_{PP-AA}$ and hZnT6, but rather that they resulted from defects of hTNAP protein maturation during the two-step mechanism, which were caused by mutating the two proline residues to alanine.

The PP-motif in luminal loop 2 of ZnT7 is crucial for TNAP activation, but not for its zinc transport activity

Next, we examined the effects of the PP-AA mutation on the zinc transport activity of hZnT5 using the yeast *msc2* mutant [43,44], which was recently used to evaluate the zinc transport activity of *Arabidopsis thaliana* ZnT5 and ZnT6 orthologues (MTP12 and MTP5 respectively) [40]. However, we failed to detect any zinc transport activity of the hZnT5$_{PP-AA}$ mutant using the *msc2* mutant under our growth conditions, because co-expression of WThZnT5 and hZnT6 did not restore the growth of the *msc2* mutant (results not shown). Instead, we examined the effects of the PP-AA mutation on the zinc transport activity of hZnT7. As described above, hZnT7 is highly homologous with hZnT5, thus the model structures of hZnT5 and hZnT7, which were generated based on the crystal structure of the *Escherichia coli* ZnT homologue YiiP [14,15,17], were well merged. We speculated that the PP-motif in both proteins protrudes into the luminal side of the membrane (Figures 3A and 3B). Then, we examined the significance of the PP-motif in hZnT7 for TNAP

activation using the same mutagenesis strategy. In a similar manner to the hZnT5 mutants, the TNAP activity in TKO cells stably expressing either single substitution mutants of hZnT7 (hZnT7$_{P133A}$ or hZnT7$_{P134A}$) was moderately reduced, and it was markedly reduced in cells stably expressing the hZnT7$_{PP-AA}$ mutant (Figure 3C). Importantly, we confirmed that the expression of the hZnT7$_{PP-AA}$ mutant, but not the hZnT7$_{H70A}$ mutant (a zinc transport-incompetent mutant), restored the growth of the *msc2* mutant in a manner that was comparable to that of WT hZnT7 (Figure 3D), indicating that zinc transport activity is not significantly impaired in the hZnT7$_{PP-AA}$ mutant. These results suggest that hZnT5$_{PP-AA}$ probably retains its zinc transport activity, and that the PP-motifs of hZnT5 and hZnT7 have important functions, except in zinc transport, during TNAP activation in the early secretory pathway.

The necessity and sufficiency of the PP-motif in ZnT5 orthologues and other ZnT transporters

The PP-motif is highly conserved in hZnT5 and hZnT7 orthologues (Tables 1 and 2), suggesting that it has a specific and important function in secretory and membrane-bound zinc-requiring enzyme activation. Therefore, we investigated whether the PP-motif is necessary and sufficient for TNAP activation. First, we examined the necessity of the PP-motif in CDF5, which is the *C. elegans* ZnT5 orthologue, because it has 15 putative TMDs [27,36], high overall sequence homology (41 % identity and 57 % similarity with hZnT5) [45], and, importantly, because its C-terminal portion [the cation efflux domain (pfam01545)] is homologous with hZnT5 (identity, 47 %; similarity, 63 %), and hZnT7 (identity, 37 %; similarity, 53 %) (note that *C. elegans* does not have a ZnT7 orthologue). Stable expression of CDF5 alone failed to restore TNAP activity in TKO cells (Figure 4A), indicating that CDF5 needs an auxiliary subunit. Therefore, we stably co-expressed CDF5 and TOC1, which was speculated to be the *C. elegans* ZnT6 orthologue in our previous studies [30,46], in TKO cells, and examined the TNAP activity. Co-expression of CDF5 and TOC1 restored TNAP activity in TKO cells to approximately 75 % of that of the case in which hZnT5 and hZnT6 were co-expressed (Figure 4A). Consistent with this, CDF5 and TOC1 co-localized to Golgi-like compartments (Figure 4B), and they formed heterodimers in a similar manner to their human counterparts (Figure 4C). TNAP activity in TKO cells stably expressing a double substitution mutant (CDF5$_{PP-AA}$) with TOC1 was markedly reduced. However, almost no effects were found in cells expressing either of the single alanine substitution mutants (CDF5$_{P499A}$ and CDF5$_{P500A}$) (Figure 4D). Hence these results confirm that the PP-motif of a ZnT5 orthologue is indispensable for appropriate TNAP activation.

Next, we investigated whether the PP-motif is sufficient to confer the ability to activate TNAP on other ZnT transporters. For this purpose, we constructed swapping mutants in which the MNY sequence of hZnT4 was mutated to the PP sequence (hZnT4$_{MNY-PP}$) or the PP sequence of hZnT5 was mutated to the MNY sequence (hZnT5$_{PP-MNY}$) (Figure 1A). The zinc transport activity of the hZnT4$_{MNY-PP}$ mutant was confirmed using $ZnT1^{-/-}\ MT^{-/-}\ ZnT4^{-/-}$ cells, which are highly sensitive to high zinc concentrations [38,39] and which is reversed by expressing WT hZnT4 [21]. Expressing the hZnT4$_{MNY-PP}$ mutant reversed the zinc sensitive phenotype of the $ZnT1^{-/-}\ MT^{-/-}\ ZnT4^{-/-}$ cells to a similar extent to that of

cells expressing WT hZnT4 (Figure 5A), indicating that the MNY-PP mutation did not impair the zinc transport activity of hZnT4. Expressing hZnT4$_{MNY-PP}$ in TKO cells, however, failed to restore TNAP activity (Figure 5B), whereas co-expressing the hZnT5$_{PP-MNY}$ mutant with hZnT6 resulted in a significant reduction of TNAP activity (Figure 5C), which is consistent with the results obtained using the hZnT5$_{PP-AA}$ mutant (Figure 2B). These results reveal that the PP-motif is important for hZnT5, hZnT7 and their orthologues, as it is a specific motif that is associated with TNAP activation, but it is not sufficient to confer the ability to activate TNAP to other ZnT transporters.

DISCUSSION

Many mutagenesis studies of cation diffusion facilitator proteins, including ZnT transporters, have been performed. For example, extensive analyses have been conducted in MTP1 in plants and Zrc1 in yeast, and they have identified a number of amino acid residues that are essential for zinc transport activity and for determining metal substrate specificity [23-26]. In vertebrate ZnTs, a few similar studies have been performed, and they confirmed the importance of the HDHD core motif in zinc transport activity and metal substrate specificity [18-22].However, investigations of the contribution of other amino acid residues to the functions of ZnTs have not been explored. In the present study, we demonstrated that the PP-motif in luminal loop 2 of hZnT5, hZnT7, and the hZnT5 orthologue CDF5 is a specific motif that is associated with TNAP activation. To our knowledge, this is the first evidence of the importance of the conserved luminal motif of ZnTs at a molecular level, and it provides novel molecular insights into enzyme activation in the early secretory pathway.

The PP-motif of luminal loop 2 is occupied by two amino acids in hZnT5, hZnT7 and CDF5, whereas three amino acids are present in other ZnT transporters (Figure 1A). Our results for the hZnT7$_{PP-AA}$ (Figure 3D) and hZnT4$_{MNY-PP}$ mutants (Figure 5A) indicate that these differences do not seem to cause significant changes in zinc transport activity, suggesting that the PP-motif is uniquely equipped to maintain a specific conformation, which leads to questions regarding its function in TNAP activation. One possibility is that the PP-motif functions as a protein-binding motif, because the proline-rich motif has an unusual secondary structure that is known to be involved in protein binding [47,48]. Our results showed that low-molecular-mass bands of hTNAP, which probably correspond to apo-hTNAP [30,35], appeared in TKO cells stably co-expressing hZnT5$_{PP-AA}$ and hZnT6 (Figures 2C and 2D), which suggests that the PP-motif may be important for protein–protein interactions in the TNAP maturation process during the two-step mechanism. We hypothesized that hZnT5 or hZnT7 may interact with hTNAP through the PP-motif, but we failed to detect a direct interaction between them (results not shown). The PP-motif may contribute to functional interactions with unknown proteins that are involved in transferring luminal zinc to TNAP for its metalation (and/or stability). If the PP-motif functions in protein–protein interactions, other regions in hZnT5 and hZnT7 would also be crucial, because the PP-motif was not sufficient to confer the ability to activate TNAP to other ZnT transporters such as hZnT4 (Figure 5B), and because TNAP activity was not completely lost in TKO cells stably expressing the hZnT5$_{PP-AA}$ mutant and hZnT6 (Figures 2B and 2D), their orthologues (Figure 4D), and the hZnT7$_{PP-AA}$ mutant (Figure 3C).

Another possibility is that proline residues in the PP-motif may be hydroxylated and that the hydroxy-proline residues might function as zinc-co-ordinating ligands or they might facilitate zinc co-ordination during TNAP activation, thus reducing TNAP activity in cells expressing the PP-AA mutants. However, this possibility was excluded because TNAP activity was not changed in WT DT40 cells that were cultured in the presence of dimethyloxalylglycine, an inhibitor of prolyl 4-hydroxylase [49] (results not shown), which mainly mediates the hydroxylation of proline in collagen [50]. This exclusion is also supported by the fact that the PP-motif in hZnT5, hZnT7 and CDF5 differs from the $(XPG)^n$ motif in collagen, which is highly hydroxylated [50].

The PP-motif in luminal loop 2 is highly conserved among ZnT5 and ZnT7 and their orthologues (Tables 1 and 2), but, interestingly, the *A. thaliana* and *S. cerevisiae* ZnT5 orthologues (MTP12 and Msc2 respectively) [40,43,51], as well as the *Xenopus tropicalis* ZnT7 orthologue, lack one of the proline residues. In these species, ZnT5 and ZnT7 orthologues with only one proline residue may be functional, as was demonstrated for CDF5$_{P499A}$ and CDF5$_{P500A}$ (Figure 4D). Moreover, the PP-motif is found in several ZnT transporter homologues that are not assigned as ZnT5 and ZnT7 orthologues in some species (Table 3). Among them, it is of interest that *S. cerevisiae* Cot1 has the PP-motif, because the *S. cerevisiae* alkaline phosphatase Pho8 is activated by Cot1 (and Zrc1) (both of which are highly homologous with ZnT4) in vacuoles, but not by Msc2 and Zrg17 (a ZnT6 homologue) [52]. The PP-motif of Cot1 may be uniquely important in the activation of Pho8 in vacuoles in *S. cerevisiae*.

The mutation of the HDHD core motif of the intramembranous zinc-binding site to DDHD or HDHE in hZnT5 impaired its TNAP activation property (see Supplementary Figure S1), although neither mutation impairs its zinc transport activity [18,20]. These results indicate that the HDHD core motif is important for ZnT transporters to mediate enzyme activation. Considering that the HDHD core motif is located just below the PP-motif in the model structures of hZnT5 and hZnT7, a unique co-operative mechanism may be responsible for proper zinc transfer from the HDHD core motif to TNAP through the PP-motif, although future investigations are needed to clarify this.

In conclusion, this is the first report describing the importance of the PP-motif and the HDHD core motif for TNAP activation in the early secretory pathway. During the activation of secretory/membrane-bound metalloenzymes, compartmentalization has been shown to be one important means of regulation [53,54]. Additionally, the present study reveals that there is another form of regulation, which is under the control of the motifs that are embedded in metal transporter sequences, such as the PP-motif and HDHD core motif. A number of physiopathologically important proteins, such as matrix metalloproteinases, angiotensin- or endothelin-converting enzymes, a disintegrin, and metalloproteinase family proteins, are all secretory/membrane-bound zinc-requiring enzymes [27,34]. Thus, clarifying the molecular basis underlying TNAP activation may give us important insights into clinical disorders that are associated with these enzymes.

Supplementary Material

Refer to Web version on PubMed Central for supplementary material.

Acknowledgments

References

1. Maret W. New perspectives of zinc coordination environments in proteins. J Inorg Biochem. 2012; 111:110–116. [PubMed: 22196021]

2. Kochanczyk T, Drozd A, Krezel A. Relationship between the architecture of zinc coordination and zinc binding affinity in proteins–insights into zinc regulation. Metallomics. 2015; 7:244–257. [PubMed: 25255078]

3. Fukada T, Kambe T. Molecular and genetic features of zinc transporters in physiology and pathogenesis. Metallomics. 2011; 3:662–674. [PubMed: 21566827]

4. Kambe T, Tsuji T, Hashimoto A, Itsumura N. The physiological, biochemical, and molecular roles of zinc transporters in zinc homeostasis and metabolism. Physiol Rev. 2015; 95:749–784. [PubMed: 26084690]

5. Andreini C, Banci L, Bertini I, Rosato A. Counting the zinc-proteins encoded in the human genome. J Proteome Res. 2006; 5:196–201. [PubMed: 16396512]

6. Kimura T, Kambe T. The functions of metallothionein and ZIP and ZnT transporters: an overview and perspective. Int J Mol Sci. 2016; 17:336. [PubMed: 26959009]

7. Kambe T, Weaver BP, Andrews GK. The genetics of essential metal homeostasis during development. Genesis. 2008; 46:214–228. [PubMed: 18395838]

8. Lichten LA, Cousins RJ. Mammalian zinc transporters: nutritional and physiologic regulation. Annu Rev Nutr. 2009; 29:153–176. [PubMed: 19400752]

9. Kambe T. Molecular architecture and function of ZnT transporters. Curr Top Membr. 2012; 69:199–220. [PubMed: 23046652]

10. Dempski RE. The cation selectivity of the ZIP transporters. Curr Top Membr. 2012; 69:221–245. [PubMed: 23046653]

11. Huang L, Tepaamorndech S. The SLC30 family of zinc transporters – a review of current understanding of their biological and pathophysiological roles. Mol Aspects Med. 2013; 34:548–560. [PubMed: 23506888]

12. Jeong J, Eide DJ. The SLC39 family of zinc transporters. Mol Aspects Med. 2013; 34:612–619. [PubMed: 23506894]

13. Kambe T, Hashimoto A, Fujimoto S. Current understanding of ZIP and ZnT zinc transporters in human health and diseases. Cell Mol Life Sci. 2014; 71:3281–3295. [PubMed: 24710731]

14. Lu M, Fu D. Structure of the zinc transporter YiiP. Science. 2007; 317:1746–1748. [PubMed: 17717154]

15. Lu M, Chai J, Fu D. Structural basis for autoregulation of the zinc transporter YiiP. Nat Struct Mol Biol. 2009; 16:1063–1067. [PubMed: 19749753]

16. Coudray N, Valvo S, Hu M, Lasala R, Kim C, Vink M, Zhou M, Provasi D, Filizola M, Tao J, et al. Inward-facing conformation of the zinc transporter YiiP revealed by cryoelectron microscopy. Proc Natl Acad Sci USA. 2013; 110:2140–2145. [PubMed: 23341604]

17. Gupta S, Chai J, Cheng J, D'Mello R, Chance MR, Fu D. Visualizing the kinetic power stroke that drives proton-coupled zinc(II) transport. Nature. 2014; 512:101–104. [PubMed: 25043033]

18. Ohana E, Hoch E, Keasar C, Kambe T, Yifrach O, Hershfinkel M, Sekler I. Identification of the Zn^{2+} binding site and mode of operation of a mammalian Zn^{2+} transporter. J Biol Chem. 2009; 284:17677–17686. [PubMed: 19366695]

19. Fukunaka A, Suzuki T, Kurokawa Y, Yamazaki T, Fujiwara N, Ishihara K, Migaki H, Okumura K, Masuda S, Yamaguchi-Iwai Y, et al. Demonstration and characterization of the heterodimerization of ZnT5 and ZnT6 in the early secretory pathway. J Biol Chem. 2009; 284:30798–30806. [PubMed: 19759014]

20. Hoch E, Lin W, Chai J, Hershfinkel M, Fu D, Sekler I. Histidine pairing at the metal transport site of mammalian ZnT transporters controls Zn^{2+} over Cd^{2+} selectivity. Proc Natl Acad Sci USA. 2012; 109:7202–7207. [PubMed: 22529353]

21. Fujimoto S, Itsumura N, Tsuji T, Anan Y, Tsuji N, Ogra Y, Kimura T, Miyamae Y, Masuda S, Nagao M, Kambe T. Cooperative functions of ZnT1, metallothionein and ZnT4 in the cytoplasm are required for full activation of TNAP in the early secretory pathway. PLoS One. 2013; 8:e77445. [PubMed: 24204829]

22. Shusterman E, Beharier O, Shiri L, Zarivach R, Etzion Y, Campbell CR, Lee IH, Okabayashi K, Dinudom A, Cook DI, et al. ZnT-1 extrudes zinc from mammalian cells functioning as a Zn(2 +)/ H(+) exchanger. Metallomics. 2014; 6:1656–1663. [PubMed: 24951051]

23. Menguer PK, Farthing E, Peaston KA, Ricachenevsky FK, Fett JP, Williams LE. Functional analysis of the rice vacuolar zinc transporter OsMTP1. J Exp Bot. 2013; (64):2871–2883. [PubMed: 23761487]

24. Podar D, Scherer J, Noordally Z, Herzyk P, Nies D, Sanders D. Metal selectivity determinants in a family of transition metal transporters. J Biol Chem. 2012; 287:3185–3196. [PubMed: 22139846]

25. Lin H, Burton D, Li L, Warner DE, Phillips JD, Ward DM, Kaplan J. Gain-of-function mutations identify amino acids within transmembrane domains of the yeast vacuolar transporter Zrc1 that determine metal specificity. Biochem J. 2009; 422:273–283. [PubMed: 19538181]

26. Kawachi M, Kobae Y, Kogawa S, Mimura T, Kramer U, Maeshima M. Amino acid screening based on structural modeling identifies critical residues for the function, ion selectivity and structure of *Arabidopsis* MTP1. FEBS J. 2012; 279:2339–2356. [PubMed: 22520078]

27. Kambe T. An overview of a wide range of functions of ZnT and Zip zinc transporters in the secretory pathway. Biosci Biotechnol Biochem. 2011; 75:1036–1043. [PubMed: 21670538]

28. Kelleher SL, McCormick NH, Velasquez V, Lopez V. Zinc in specialized secretory tissues: roles in the pancreas, prostate, and mammary gland. Adv Nutr. 2011; 2:101–111. [PubMed: 22332039]

29. Hennigar SR, Kelleher SL. Zinc networks: the cell-specific compartmentalization of zinc for specialized functions. Biol Chem. 2012; 393:565–578. [PubMed: 22944660]

30. Ishihara K, Yamazaki T, Ishida Y, Suzuki T, Oda K, Nagao M, Yamaguchi-Iwai Y, Kambe T. Zinc transport complexes contribute to the homeostatic maintenance of secretory pathway function in vertebrate cells. J Biol Chem. 2006; 281:17743–17750. [PubMed: 16636052]

31. Suzuki T, Ishihara K, Migaki H, Nagao M, Yamaguchi-Iwai Y, Kambe T. Two different zinc transport complexes of cation diffusion facilitator proteins localized in the secretory pathway operate to activate alkaline phosphatases in vertebrate cells. J Biol Chem. 2005; 280:30956–30962. [PubMed: 15994300]

32. Lasry I, Golan Y, Berman B, Amram N, Glaser F, Assaraf YG. *In situ* dimerization of multiple wild type and mutant zinc transporters in live cells using bimolecular fluorescence complementation. J Biol Chem. 2014; 289:7275–7292. [PubMed: 24451381]

33. Suzuki T, Ishihara K, Migaki H, Matsuura W, Kohda A, Okumura K, Nagao M, Yamaguchi-Iwai Y, Kambe T. Zinc transporters, ZnT5 and ZnT7, are required for the activation of alkaline phosphatases, zinc-requiring enzymes that are glycosylphosphatidylinositol-anchored to the cytoplasmic membrane. J Biol Chem. 2005; 280:637–643. [PubMed: 15525635]

34. Kambe T, Takeda T, Nishito Y. Activation of zinc-requiring ectoenzymes by ZnT transporters during the secretory process: Biochemical and molecular aspects. Arch Biochem Biophys. 2016; doi: 10.1016/j.abb.2016.03.035

35. Fukunaka A, Kurokawa Y, Teranishi F, Sekler I, Oda K, Ackland ML, Faundez V, Hiromura M, Masuda S, Nagao M, et al. Tissue nonspecific alkaline phosphatase is activated via a two-step mechanism by zinc transport complexes in the early secretory pathway. J Biol Chem. 2011; 286:16363–16373. [PubMed: 21402707]

36. Kambe T, Narita H, Yamaguchi-Iwai Y, Hirose J, Amano T, Sugiura N, Sasaki R, Mori K, Iwanaga T, Nagao M. Cloning and characterization of a novel mammalian zinc transporter, zinc transporter 5, abundantly expressed in pancreatic beta cells. J Biol Chem. 2002; 277:19049–19055. [PubMed: 11904301]

37. Kambe T. Methods to evaluate zinc transport into and out of the secretory and endosomal–lysosomal compartments in DT40 cells. Methods Enzymol. 2014; 534:77–92. [PubMed: 24359949]

38. Itsumura N, Inamo Y, Okazaki F, Teranishi F, Narita H, Kambe T, Kodama H. Compound heterozygous mutations in SLC30A2/ZnT2 results in low milk zinc concentrations: a novel mechanism for zinc deficiency in a breast-fed infant. PLoS One. 2013; 8:e64045. [PubMed: 23741301]

39. Itsumura N, Kibihara Y, Fukue K, Miyata A, Fukushima K, Tamagawa-Mineoka R, Katoh N, Nishito Y, Ishida R, Narita H, et al. Novel mutations in SLC30A2 involved in the pathogenesis of transient neonatal zinc deficiency. Pediatr Res. 2016; doi: 10.1038/pr.2016.108

40. Fujiwara T, Kawachi M, Sato Y, Mori H, Kutsuna N, Hasezawa S, Maeshima M. A high molecular mass zinc transporter MTP12 forms a functional heteromeric complex with MTP5 in the Golgi in *Arabidopsis thaliana*. FEBS J. 2015; 282:1965–1979. [PubMed: 25732056]

41. Rai BK, Fiser A. Multiple mapping method: a novel approach to the sequence-to-structure alignment problem in comparative protein structure modeling. Proteins. 2006; 63:644–661. [PubMed: 16437570]

42. Gietz RD, Woods RA. Transformation of yeast by lithium acetate/single-stranded carrier DNA/polyethylene glycol method. Methods Enzymol. 2002; 350:87–96. [PubMed: 12073338]

43. Li L, Kaplan J. The yeast gene MSC2, a member of the cation diffusion facilitator family, affects the cellular distribution of zinc. J Biol Chem. 2001; 276:5036–5043. [PubMed: 11058603]

44. Ellis CD, Macdiarmid CW, Eide DJ. Heteromeric protein complexes mediate zinc transport into the secretory pathway of eukaryotic cells. J Biol Chem. 2005; 280:28811–28818. [PubMed: 15961382]

45. Kambe T, Suzuki T, Nagao M, Yamaguchi-Iwai Y. Sequence similarity and functional relationship among eukaryotic ZIP and CDF transporters. Genomics Proteomics Bioinformatics. 2006; 4:1–9. [PubMed: 16689696]

46. Ewbank JJ, Barnes TM, Lakowski B, Lussier M, Bussey H, Hekimi S. Structural and functional conservation of the *Caenorhabditis elegans* timing gene clk-1. Science. 1997; 275:980–983. [PubMed: 9020081]

47. Tu JC, Xiao B, Yuan JP, Lanahan AA, Leoffert K, Li M, Linden DJ, Worley PF. Homer binds a novel proline-rich motif and links group 1 metabotropic glutamate receptors with IP3 receptors. Neuron. 1998; 21:717–726. [PubMed: 9808459]

48. Zarrinpar A, Bhattacharyya RP, Lim WA. The structure and function of proline recognition domains. Sci STKE. 2003; 2003:RE8. [PubMed: 12709533]

49. Kalson NS, Starborg T, Lu Y, Mironov A, Humphries SM, Holmes DF, Kadler KE. Nonmuscle myosin II powered transport of newly formed collagen fibrils at the plasma membrane. Proc Natl Acad Sci USA. 2013; 110:E4743–E4752. [PubMed: 24248360]

50. Gorres KL, Raines RT. Prolyl 4-hydroxylase. Crit Rev Biochem Mol Biol. 2010; 45:106–124. [PubMed: 20199358]

51. Ellis CD, Wang F, MacDiarmid CW, Clark S, Lyons T, Eide DJ. Zinc and the Msc2 zinc transporter protein are required for endoplasmic reticulum function. J Cell Biol. 2004; 166:325–335. [PubMed: 15277543]

52. Qiao W, Ellis C, Steffen J, Wu CY, Eide DJ. Zinc status and vacuolar zinc transporters control alkaline phosphatase accumulation and activity in *Saccharomyces cerevisiae*. Mol Microbiol. 2009; 72:320–334. [PubMed: 19298366]

53. Setty SR, Tenza D, Sviderskaya EV, Bennett DC, Raposo G, Marks MS. Cell-specific ATP7A transport sustains copper-dependent tyrosinase activity in melanosomes. Nature. 2008; 454:1142–1146. [PubMed: 18650808]

54. Tottey S, Waldron KJ, Firbank SJ, Reale B, Bessant C, Sato K, Cheek TR, Gray J, Banfield MJ, Dennison C, Robinson NJ. Protein-folding location can regulate manganese-binding versus copper- or zinc-binding. Nature. 2008; 455:1138–1142. [PubMed: 18948958]

Abbreviations

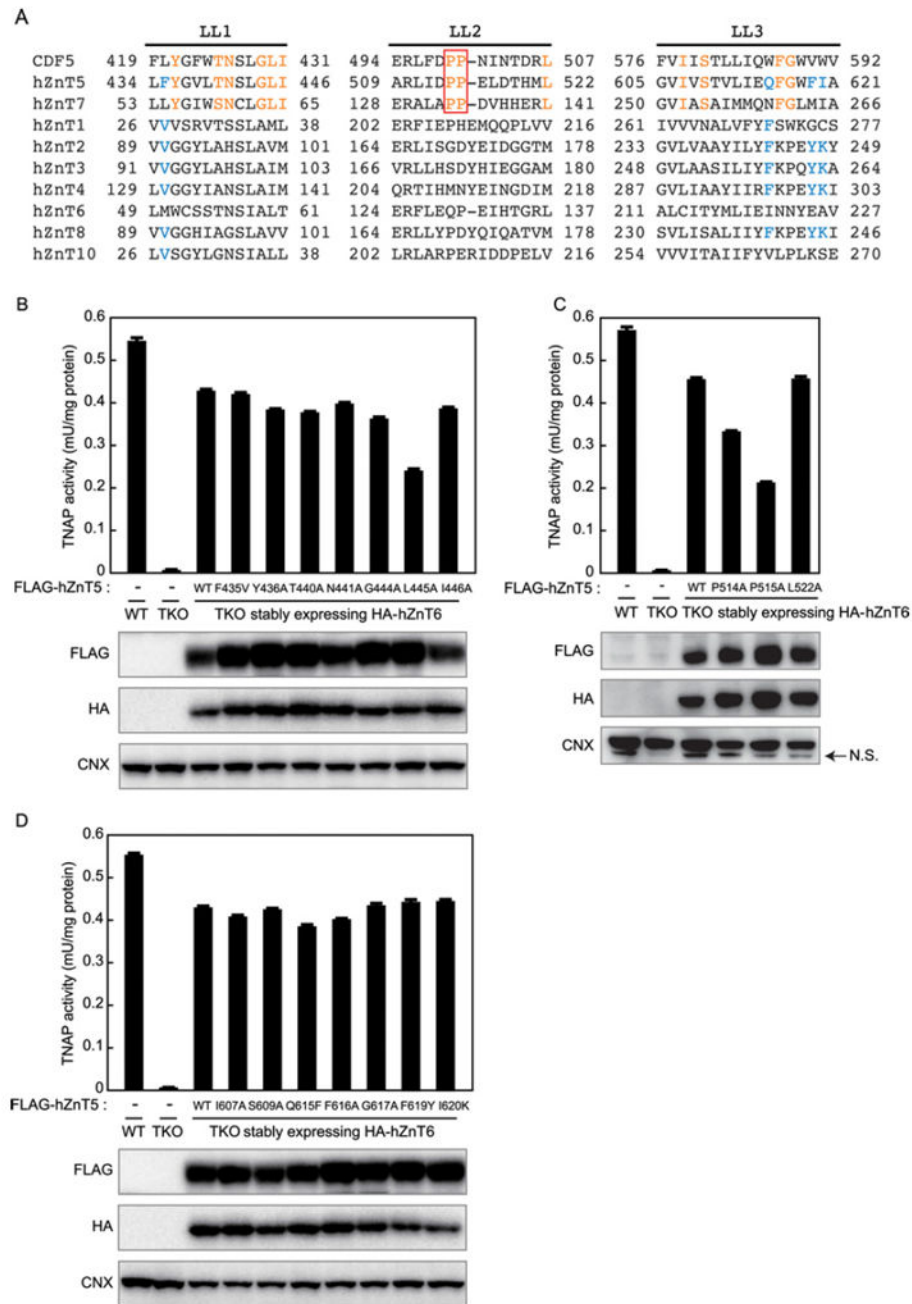|	
HA	haemagglutinin
hZnT	human ZnT
MT	metallothionein
SLC	solute carrier
TKO	triple knockout
TMD	transmembrane domain
TNAP	tissue-non-specific alkaline phosphatase
WT	wild-type
ZIP	Zrt, Irt-like protein
ZnT	zinc transporter

Figure 1. Evaluation of the involvement of amino acids in the luminal loops of hZnT5 in TNAP activation

(**A**) Sequence alignment of luminal loops among CDF5, hZnT5, hZnT7 and other human ZnT transporters. The sequences used for alignment are shown in the Supplementary Online Data. In hZnT5 and CDF5, luminal loops 5, 6 and 7 correspond to luminal loops 1, 2 and 3 in the other transporters. The PP-motif is boxed in red. Conserved amino acids among hZnT5, hZnT7 and CDF5, which were subjected to alanine-scanning mutagenesis, are indicated in orange. The amino acid residues in hZnT5, which were subjected to the

substitution mutagenesis, are shown in blue (substituted amino acids are also shown in blue for ZnT transporters other than hZnT5, hZnT7 and CDF5 for easy comparison). The PP-motif is boxed in red. LL, luminal loop. (**B**) Effects of alanine-scanning and substitution mutagenesis of amino acid residues in luminal loop 1 of hZnT5 on TNAP activation. (**C**) Effects of alanine-scanning mutagenesis of amino acid residues in luminal loop 2 of hZnT5 on TNAP activation. (**D**) Effects of alanine-scanning and substitution mutagenesis of amino acid residues in luminal loop 3 of hZnT5 on TNAP activation. In (**B**)–(**D**), the amino acids of hZnT5 that are indicated in (**A**) were mutated (see the text). TNAP activity in TKO cells stably co-expressing each hZnT5 mutant with hZnT6 was measured, and it is expressed as the mean ± S.D. for three independent experiments. Expression of all of the hZnT5 mutants and hZnT6 was confirmed by immunoblotting (lower panels). Calnexin (CNX) is shown as a loading control. N.S., non-specific.
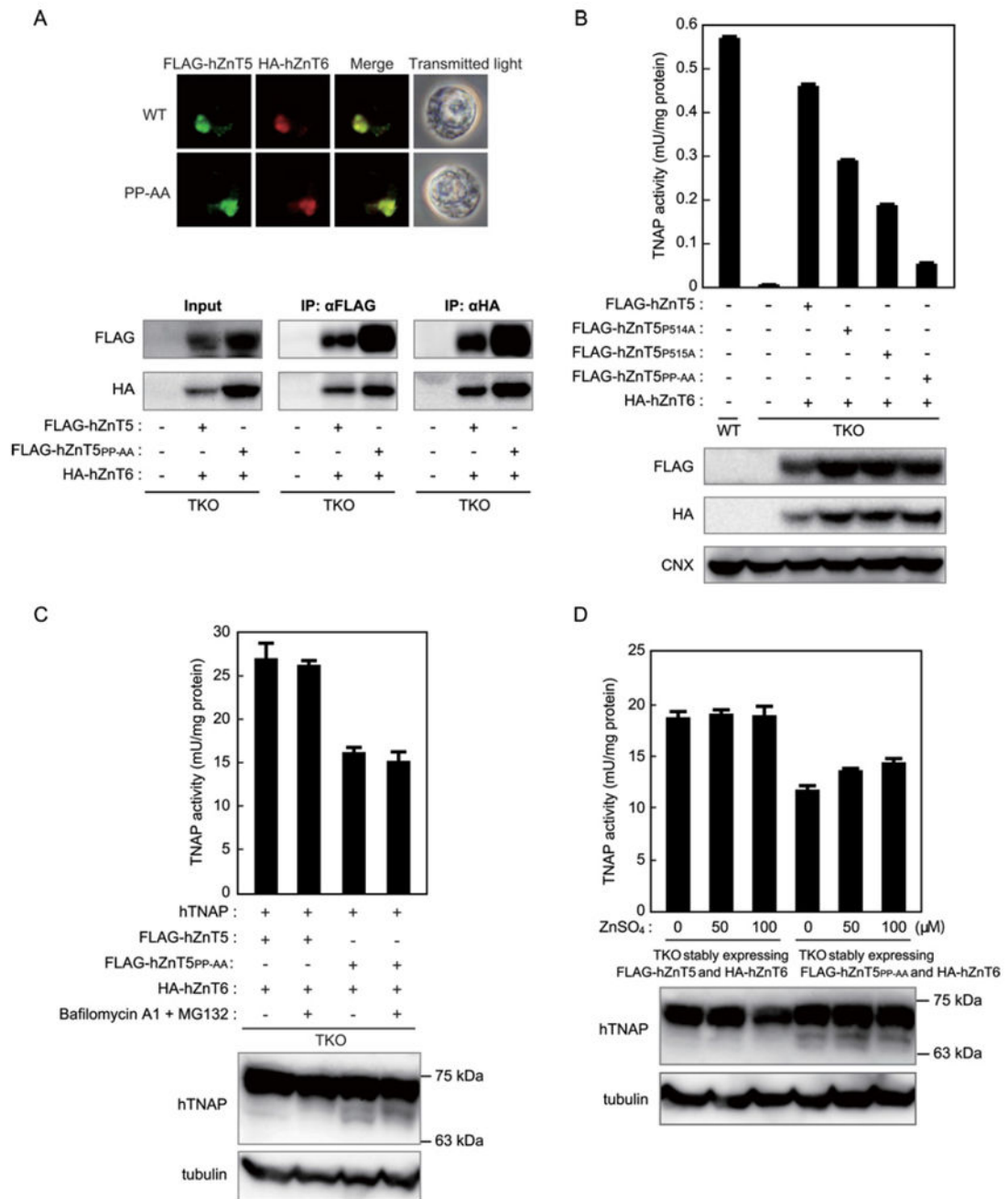
Figure 2. The PP-motif in luminal loop 2 of hZnT5 is crucial for TNAP activation

(**A**) The hZnT5$_{PP-AA}$ mutant co-localizes with hZnT6 and forms heterodimers with hZnT6 just like WT hZnT5. Stably expressed FLAG-hZnT5 or the FLAG-hZnT5$_{PP-AA}$ mutant and HA-hZnT6 were double-stained (upper panels). Membrane proteins were prepared from TKO cells, and FLAG-hZnT5 and HA-hZnT6 were immunoprecipitated with antibodies against the FLAG and HA tags respectively (lower panels). A 12% sample of each aliquot was subjected to an immunoblot analysis (input). (**B**) The PP-motif in luminal loop 2 of hZnT5 is crucial for TNAP activation. TNAP activity in the indicated cells was measured as

in Figure 1(B), and it is expressed as the mean ± S.D. for three independent experiments. Expression of each protein was confirmed by immunoblotting (lower panels). Calnexin (CNX) is shown as a loading control. (**C**) A minor low-molecular-mass band of the hTNAP protein appears in TKO cells stably expressing ZnT5PP-AA with hZnT6, but not WT hZnT5. The TNAP activity (the sum of the exogenously expressed hTNAP plus endogenous TNAP) was measured using total cellular proteins that were prepared from the indicated cells (upper panel). hTNAP was detected as one high-molecular-mass band of ~75-kDa (in the case of WT hZnT5) or one major band (~75-kDa) and minor ~65-kDa bands (in the case of ZnT5$_{PP-AA}$). The ~65-kDa bands were not significantly changed by the treatment with both MG132 (30 μM) and bafilomycin A1 (30 nM) for 2 h (lower panel). (D) Zinc supplementation did not significantly restore hTNAP activity, and it did not cause the ~65-kDa bands to disappear. TNAP activity was measured using total cellular proteins that were prepared from cells cultured with 50 or 100 μM ZnSO$_4$ for 24 h, as in (C) (upper panel). In (C) and (D), the TNAP activity is expressed as the mean ± S.D. for triplicate experiments. A 20 μg amount of total cellular protein was loaded in each lane. Tubulin is shown as a loading control. The positions of the protein size markers are indicated on the right.
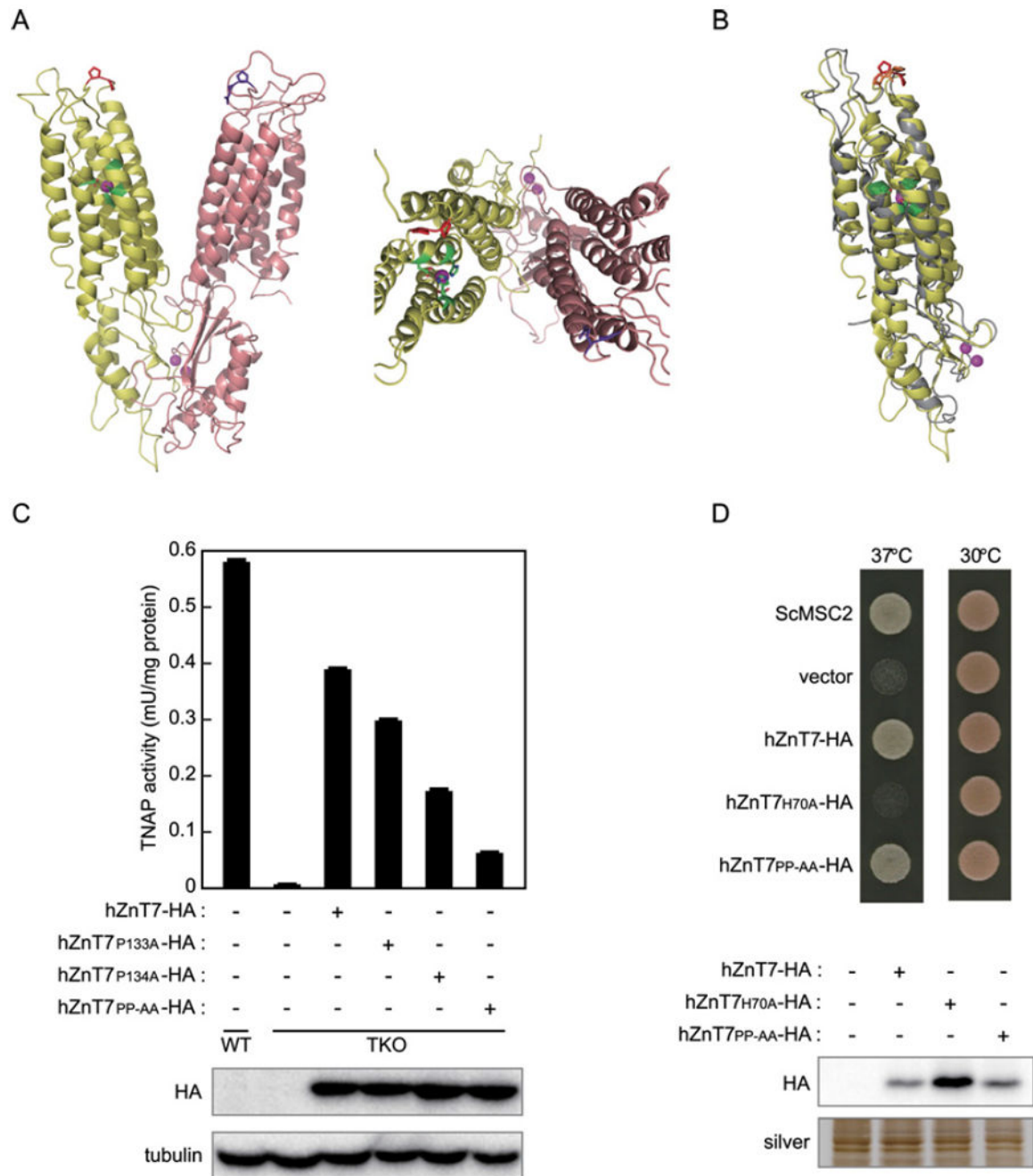
Figure 3. The PP-motif in luminal loop 2 of hZnT7 is crucial for TNAP activation

(**A**) Ribbon representation of the 3D model of hZnT5–hZnT6 heterodimer (left, view from the membrane plane; right, view from the extracellular side). hZnT5 (only the cation efflux domain) and hZnT6 are in yellow and salmon respectively. The PP-motif and the intramembranous zinc-binding site are shown in red and green respectively. The corresponding position of hZnT6 is shown in aubergine. Purple circle, zinc ion. (**B**) Ribbon representation of the 3D model of hZnT5 and hZnT7. The hZnT5 monomer (only the cation efflux domain) is overlaid on the hZnT7 monomer, which are in yellow and grey

respectively. The PP-motifs are shown in red (for hZnT5) and orange (for hZnT7), and the intramembranous zinc-binding sites are shown in green. Purple circle, zinc ion. (**C**) The PP-motif in luminal loop 2 of hZnT7 is crucial for TNAP activation. TNAP activity in the indicated cells was measured as in Figure 1(B). Expression of the hZnT7 mutants was confirmed by immunoblotting (lower panels). Tubulin is shown as a loading control. (**D**) Complementation analysis of the hZnT7$_{PP-AA}$ mutant using the *S. cerevisiae* mutant DY150 *msc2* . The *msc2* mutant was transformed with pYES2 vectors containing the *ScMSC2*, *hZnT7-HA*, *hZnT7$_{H70A}$-HA* or *hZnT7$_{PP-AA}$-HA* genes. The YPGEgal plates, on which transformed yeast cells were plated, were incubated for 3 days at 30 and 37 °C (upper panel). The expression of each ZnT7 mutant was confirmed by immunoblotting (lower panel). A silver-stained gel is shown as a loading control. A 1 μg sample of membrane protein was loaded in each lane for the immunoblotting and silver staining.
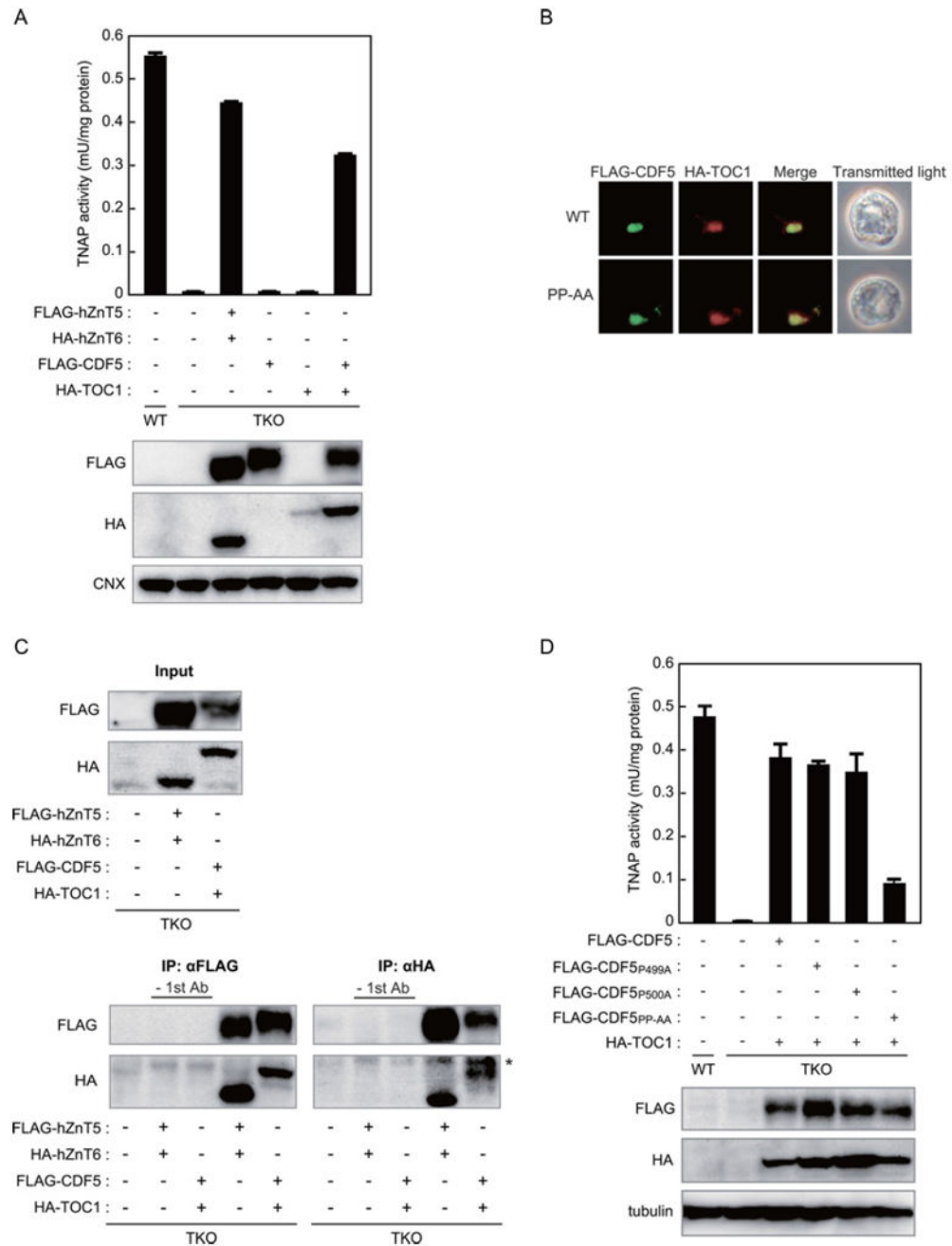
Figure 4. *C. elegans* CDF5 and TOC1 restore TNAP activity in TKO cells, but the PP-AA mutant of CDF5 does not

(**A**) Co-expression of CDF5 and TOC1, but not the expression of CDF5 or TOC1 alone, restores TNAP activity in TKO cells (upper panel). The TNAP activity of membrane protein fractions that were prepared from the indicated cells is expressed as the mean ± S.D. for three independent experiments. The expression of FLAG-CDF5 and HA-TOC1 was confirmed by immunoblot analysis using membrane proteins that were prepared from the indicated cells (lower panels). TKO cells co-expressing FLAG-hZnT5 and HA-hZnT6 were

used as a positive control. Calnexin (CNX) is shown as a loading control. (**B**) The CDF5$_{PP-AA}$ mutant co-localizes with TOC1, as do WT hZnT5 and hZnT6. Stably expressed FLAG-CDF5 (upper panels) or the FLAG-CDF5$_{PP-AA}$ mutant (lower panels) and HA-TOC1 were double-stained. (**C**) CDF5 and TOC1 physically interact with each other. FLAG-CDF5 and HA-TOC1 were immunoprecipitated with antibodies against the FLAG and HA epitopes respectively. A 12% sample of each aliquot was subjected to an immunoblot analysis (input). Any specific bands were not detected without using the first (primary) antibody (lanes of '-1st Ab'). TKO cells co-expressing FLAG-hZnT5 and HA-hZnT6 were used as a positive control. (**D**) The PP-motif in luminal loop 2 of CDF5 is crucial for TNAP activation. TNAP activity in the indicated cells was measured as in (**A**). Expression of CDF5 mutants and TOC1 was confirmed by immunoblotting (lower panels). Tubulin is shown as a loading control.
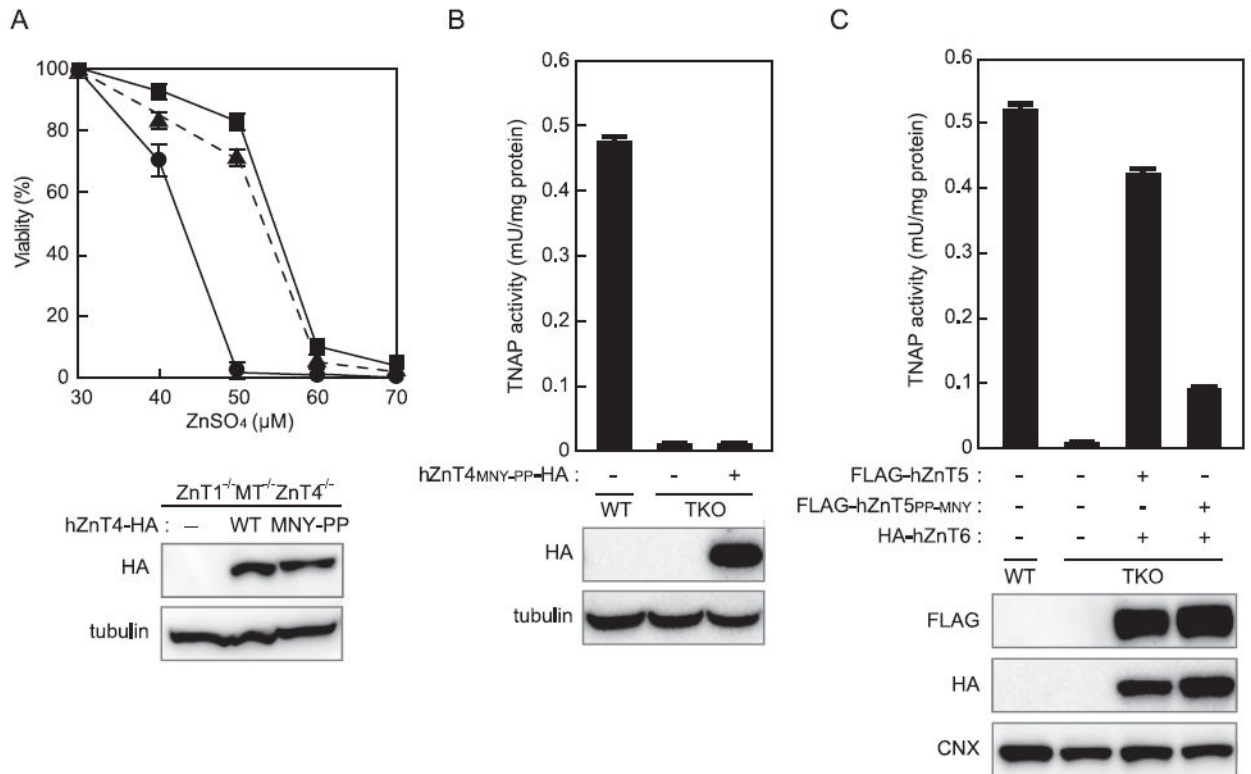
Figure 5. The PP-motif is not sufficient to confer the ability to activate TNAP to other ZnT transporters

(**A**) Evaluation of the zinc transport activity of hZnT4 mutants using $ZnT1^{-/-} MT^{-/-} ZnT4^{-/-}$ cells. $ZnT1^{-/-} MT^{-/-} ZnT4^{-/-}$ cells stably expressing WT hZnT4 or the hZnT4$_{MNY-PP}$ mutant were grown in the presence of the indicated concentrations of ZnSO$_4$ for 72 h, and the number of living cells was measured by the Alamar Blue assay (and plotted as a percentage of living cells at 30 μM ZnSO$_4$ for each group of cells). $ZnT1^{-/-} MT^{-/-} ZnT4^{-/-}$ cells (●) and $ZnT1^{-/-} MT^{-/-} ZnT4^{-/-}$ cells stably expressing WT hZnT4 (■) or hZnT4$_{MNY-PP}$ (▲). Each value is the mean ± S.D. for three independent experiments. (**B**) TNAP activity in TKO cells is not restored by expressing the hZnT$_{4MNY-PP}$ mutant. (**C**) TNAP activity is significantly reduced in TKO cells co-expressing the hZnT5$_{PP-MNY}$ mutant with hZnT6. In (**B**) and (**C**), TNAP activity is expressed as the mean ± S.D. for three independent experiments. The expression of each ZnT protein was confirmed by immunoblotting (lower panels). Tubulin and calnexin (CNX) are shown as loading controls.

Table 1

Conservation of the PP motif among ZnT5 orthologues

The accession numbers of the sequences used are shown in the Supplementary Online Data. Proline residues in the PP-motif are shown in bold.

ZnT5 orthologue	Amino acid sequence	Species
ZnT5	A^{510}RLID**PP**ELDTHML^{523}	*Homo sapiens*
ZnT5	A^{507}RLID**PP**ELDTNML^{520}	*Mus musculus*
ZnT5	A^{506}RLVD**PP**DIDTNML^{519}	*Gallus gallus*
ZnT5	A^{505}RIYD**PP**DINTDML^{518}	*X. tropicalis*
ZnT5	T^{505}RLVD**PP**NINTDML^{518}	*Danio rerio*
CDF5	E^{494}RLFD**PP**NINTDRL^{407}	*C. elegans*
Cis4	Y^{440}RLFH**PP**QMNTDQL^{453}	*Schizosaccharomyces pombe*
Msc2	E^{478}RIFN**P**IHLHATNE^{491}	*S. cerevisiae*
MTP12	E^{510}RILD**P**QEISTNSL^{523}	*A. thaliana*

Table 2

Conservation of the PP motif among ZnT7 orthologues

The accession numbers of the sequences used are shown in the Supplementary Online Data. Proline residues in the PP-motif are shown in bold.

ZnT7 orthologue	Amino acid sequence	Species
ZnT7	E^{128}RALA**PP**DVHHERL^{141}	*H. sapiens*
ZnT7	E^{128}RALA**PP**DVHHERL^{141}	*M. musculus*
ZnT7	E^{128}RALE**PP**DVHHERL^{141}	*G. gallus*
ZnT7	E^{128}RALDT**P**EVHHERL^{141}	*X. tropicalis*
ZnT7	E^{128}RALE**PP**DVHHDRL^{141}	*D. rerio*
ZnT86D	E^{126}RLIE**PP**EVKHERL^{139}	*Drosophila melanogaster*

Table 3

Distribution of the PP motif in luminal loop 2 in ZnT homologues other than ZnT5 and ZnT7

The accession numbers of the sequences used are shown in the Supplementary Online Data. Proline residues in the PP-motif are shown in bold.

CDF protein	Amino acid sequence	Species
Cot1	Q^{101}RIIA**PP**VIENPKF^{114}	*S. cerevisiae*
Zhf1	E^{101}RFIE**PP**SVSNPTL^{114}	*S. pombe*
CzcD	E^{104}RFSN**PP**KVATTGM^{117}	*Bacillus subtilis*